Transition State Imbalances in Gas Phase Proton Transfers. *Ab Initio* Study of the Carbon-to-Carbon Proton Transfer from the Protonated Acetaldehyde Cation to Acetaldehyde Enol

Claude F. Bernasconi* and Philip J. Wenzel

Contribution from the Department of Chemistry and Biochemistry, University of California, Santa Cruz, California 95064

Received January 23, 1996[⊗]

Abstract: The identity carbon-to-carbon proton transfer between oxygen-protonated acetaldehyde (syn and anti) and acetaldehyde enol (syn and anti) has been studied by *ab initio* methods at the 6-311+G**//6-311+G**, MP2/6-311+G**//6-311+G**, and MP2/6-311+G**//MP2/6-311+G** levels. Previous calculations on the proton transfer between acetaldehyde and its enolate ion have been extended to the MP2/6-311+G**//MP2/6-311+G** level. On the basis of Mulliken and natural population analysis charges, the transition states of all reactions under study show a strong imbalance in the sense that charge shift in the product enol lags behind proton transfer and charge shift in the reactant enol is ahead of proton transfer. The imbalance in the reactions of $CH_3CH{=}OH^+$ is larger than in the reaction of $CH_3CH{=}O$, and larger for the syn than the anti configuration of $CH_3CH{=}OH^+$. At the highest level of calculation, the enthalpy difference, ΔH, between the transition state and separated reactants is about −5 kcal/mol (anti) and −2 kcal/mol (syn) for the reactions of $CH_3CH{=}OH^+$, which compares with $\Delta H \approx 0$ kcal/mol for the aldehyde reaction. When basis set superposition error corrections are applied, these ΔH values become −2.6, 0.5, and 3.3 kcal/mol, respectively. The trend in these ΔH values can be understood mainly as the result of an interplay between the effect of the increased acidity of the carbon acid, which makes ΔH more negative, and the effect of a large imbalance, which makes ΔH less negative or more positive. Electrostatic or hydrogen-bonding stabilization of the transition state is also likely to play a role by attenuating these effects. Specifically, the lower ΔH for the reactions of $CH_3CH{=}OH^+$ compared to $CH_3CH{=}O$ is attributed to the much stronger acidity of $CH_3CH{=}OH^+$ which more than offsets the effect of the larger imbalance and the loss of electrostatic or hydrogen-bonding stabilization; on the other hand, the higher ΔH for the reaction of $CH_3CH{=}OH^+$ (syn) compared to that of $CH_3CH{=}OH^+$ (anti) can be explained by the dominance of the imbalance factor. The reaction paths through the imbalanced transition states can be represented by means of a six-corner More O'Ferrall−Jencks type diagram with separate axes for proton transfer and electronic/structural reorganization. The larger imbalance for the reaction of $CH_3CH{=}OH^+$ (syn) compared to $CH_3CH{=}OH^+$ (anti) is consistent with the relative energies of the intermediate corners of the diagram in the two reactions, but this is not the case for the larger imbalance in the reactions of $CH_3CH{=}OH^+$ compared to that of $CH_3CH{=}O$. This latter discrepancy is probably a consequence of an overinterpretation of the More O'Ferrall−Jencks diagram when applied to large perturbations.

Introduction

In a recent paper[1] we described an *ab initio* study of the carbon-to-carbon identity proton transfer from acetaldehyde to its enolate ion, eq 1. A major motivation for that study was to

$$O{=}CH{-}CH_3 + CH_2{=}CH{-}O^- \rightleftharpoons {}^-O{-}CH{=}CH_2 + CH_3{-}CH{=}O \quad (1)$$

examine to what extent transition state imbalances[2] commonly observed in proton transfers from carbon acids in solution also occur in the gas phase. An understanding of these imbalances and their origin is important because there is a strong correlation between transition state imbalances and intrinsic barriers or intrinsic rate constants[5] of chemical reactions in general; i.e., imbalances typically lead to higher intrinsic barriers or smaller intrinsic rate constants.[4−6]

According to our calculations, the transition state for eq 1 is indeed imbalanced in the sense that charge delocalization into the carbonyl group of the incipient *product* enolate ion lags behind proton transfer, or charge localization on the α-carbon of the *reactant* enolate ion is ahead of proton transfer.

In an attempt to quantify the degree of imbalance, we applied eq 2 to the calculated charge distribution in the transition state.

$$\delta_Y = \chi(\delta_C + \delta_Y)^n \quad (2)$$

Equation 2, which is based on a model originally proposed by Kresge[7] and later refined by us,[4,6b] refers to the generalized representation of a proton abstraction from a carbon acid activated by a π-acceptor group Y as shown in eq 3.[8] Applied to eq 1, Y represents the CHO moiety and C the CH_2 moiety of the reactant aldehyde/product enolate ion, while B is the CH_2-

⊗ Abstract published in *Advance ACS Abstracts,* October 15, 1996.

(1) Bernasconi, C. F.; Wenzel, P. J. *J. Am. Chem. Soc.* **1994**, *116*, 5405.

(2) The term imbalance is generally used to describe a situation where various processes such as bond formation/bond cleavage, development or destruction of charge and π-overlap (resonance), solvation/desolvation, etc. have made unequal progress or have developed nonsynchronously at the transition state.[3,4]

(3) (a) Jencks, D. A.; Jencks, W. P. *J. Am. Chem. Soc.* **1977**, *99*, 7948. (b) Jencks, W. P. *Chem. Rev.* **1985**, *85*, 511.

(4) For a recent review, see: Bernasconi, C. F. *Adv. Phys. Org. Chem.* **1992**, *27*, 116.

(5) For a reaction with a forward rate constant k_1 and a reverse rate constant k_{-1} the intrinsic rate constant, k_o (intrinsic barrier, $\Delta G_o^{\ddagger}$) is defined as $k_o = k_1 = k_{-1}$ when $K_1 = k_1/k_{-1} = 1$ ($\Delta G_o^{\ddagger} = \Delta G_1^{\ddagger} = \Delta G_{-1}^{\ddagger}$ when $\Delta G^\circ = 0$). In proton transfers statistical factors are sometimes included.

(6) (a) Bernasconi, C. F. *Acc. Chem. Res.* **1987**, *20*, 301. (b) Bernasconi, C. F. *Acc. Chem. Res.* **1992**, *25*, 9.

S0002-7863(96)00233-8 CCC: $12.00

$$B^{\nu} + H{-}C{-}Y \rightarrow \begin{bmatrix} \nu+\delta_B & \delta_H & -\delta_C & -\delta_Y \\ B\text{- - -}H\text{- - -}C & & & Y \end{bmatrix}^{\ddagger} \rightarrow BH^{\nu+1} + \begin{matrix} -1+\chi & -\chi \\ C & Y \end{matrix} \quad (3)$$

CHO moiety of the reactant enolate ion/product aldehyde. Note that for the case where the transferred proton carries no charge ($\delta_H = 0$) we have $\delta_C + \delta_Y = \delta_B$, but when $\delta_H \neq 0$ the relationship $\delta_C + \delta_Y = \delta_B + \delta_H$ holds.

In terms of the partial charges defined in eq 3, a transition state imbalance in the sense that charge delocalization into Y lags behind proton transfer is characterized by $\delta_Y/\delta_C < \chi/(1 - \chi)$ or $n > 1$, while a balanced transition state would lead to $\delta_Y/\delta_C = \chi/(1 - \chi)$ or $n = 1$. The degree to which n exceeds unity is a convenient measure of the size of the imbalance. Application of eq 2 to the charge distributions obtained for reactants, products, and the transition state of eq 1 suggested an n value around 1.7, implying a substantial degree of imbalance. Very similar charge distributions were also reported by Saunders[9] for the same system although they were not couched in terms of eq 2.

Another objective of our *ab initio* study was to examine the consequence of artificially reducing the imbalance by constraining the α-carbons of the transition state to a planar geometry, thereby facilitating charge delocalization into the CHO group and presumably stabilizing the transition state. Despite this resonance stabilization, the calculated reaction barrier based on this less imbalanced transition state ("trans-anti TS")[10] was 10.5 kcal/mol higher than that based on the fully optimized, more imbalanced transition state ("cis-gauche TS").[1] The lower energy of the cis-gauche TS was attributed to an electrostatic or H-bonding stabilization which results from a larger positive charge on the transferred proton (δ_H) and a larger negative charge on the CH_2 fragments (δ_C).

We now present the results of a study of the effect of adding a proton to both reactants which converts eq 1 into the carbon-to-carbon proton transfer from the oxygen-protonated acetaldehyde to the acetaldehyde enol, eq 4. Of particular interest is

$$^{+}HO{=}CH{-}CH_3 + CH_2{=}CH{-}OH \rightleftharpoons HO{-}CH{=}CH_2 + CH_3{-}CH{=}OH^{+} \quad (4)$$

how this change affects the degree of imbalance and the height of the reaction barrier. It should be noted that eq 4 is a hypothetical reaction in the sense that in an experimental situation it is likely that the O-to-O or O-to-C proton transfer would be more favorable than the C-to-C proton transfer.

Results and Discussion

The calculations were performed at the 6-311+G**//6-311+G**, MP2/6-311+G**//6-311+G**, and MP2/6-311+G**//MP2/6-311+G** levels. For better comparison with the earlier aldehyde/enolate ion study,[1] which was carried out only at the 6-311+G**//6-311+G** and MP2/6-311+G**//6-311+G** levels, we now also report results at the MP2/6-311+G**//MP2/6-311+G** level for the aldehyde system. With respect to this latter system three different transition states have been reported: the fully optimized cis-gauche TS[1,9a] and the constrained trans-anti TS[10] mentioned in the Introduction, and a fully optimized trans-anti TS.[9] At the computational levels used by Saunders,[9a] the cis-gauche TS was found to be approximately 0.1 kcal/mol more stable than the optimized trans-anti TS. However, at the MP2/6-311+G**//MP2/6-311+G** level we find the optimized trans-anti TS to be more stable than the cis-gauche TS by about 0.8 kcal/mol.[11] In the present study we therefore focus on this optimized trans-anti TS.

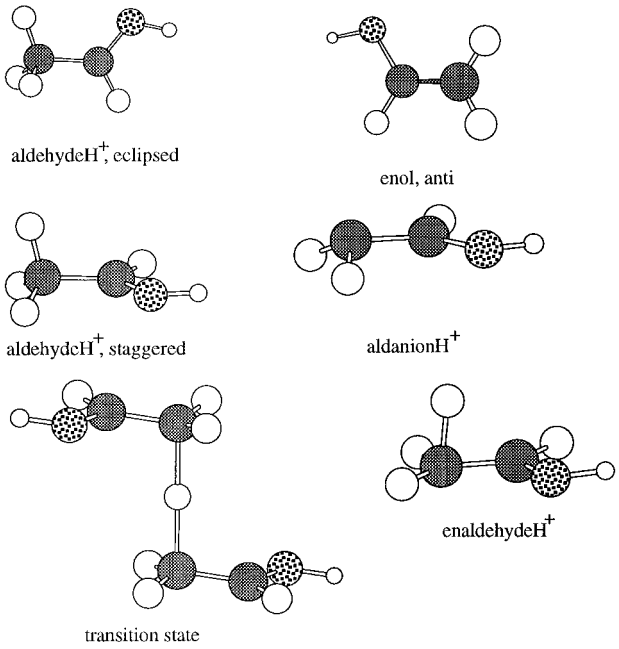

Figure 1. 3-D representations of the various structures relevant to the $CH_3CH{=}OH^+/CH_2{=}CHOH$ system (anti configuration).

3-D representations of various species relevant to eq 4 are shown in Figures 1 and 2. The geometric parameters of all the species relevant to both eqs 4 and 1 are summarized in Figures 1S, 2S, and 3S[12] of the supporting information,[13] their absolute energies are reported in Table 1S,[13] and reaction energies and reaction barriers are summarized in Table 1. Applying the counterpoise method,[14] we have also calculated basis set superposition errors (BSSE) for the various transition states. In view of the lack of agreement about the validity of such corrections,[15] the absolute transition state energies (Table 1S) and the reaction barriers (Table 1) are reported with and without such corrections.

(7) Kresge, A. J. *Can. J. Chem.* **1974**, *52*, 1897.

(8) The simplest version of eq 2 for which $n = 2$ can be derived by making the following assumptions: (1) At the transition state, the total negative charge on the C−Y moiety ($\delta_C + \delta_Y$) is distributed between C and Y in such a way that the charge on Y (δ_Y) is equal to the total charge on the C−Y moiety multiplied by the π-bond order of the C−Y bond, i.e., $\delta_Y = \pi_{bo}(\delta_C + \delta_Y)$. (2) the π-bond order, in turn, is proportional to $\delta_C + \delta_Y$, with the proportionality constant, χ, being equal to the charge on Y in the product ion, i.e., $\pi_{bo} = \chi(\delta_C + \delta_Y)$. This leads to eq 2 with $n = 2$. As pointed out by Kresge,[7] direct proportionality between delocalization and π-bond order, or between π-bond order and $\delta_C + \delta_Y$, does not necessarily apply, in which case n may be >2 or <2.

(9) (a) Saunders, W. H., Jr. *J. Am. Chem. Soc.* **1994**, *116*, 5400. (b) Saunders, W. H., Jr.; Van Verth, J. E. *J. Org. Chem.* **1995**, *60*, 3452.

(10) It should be noted that this constrained trans-anti TS is not a "true" transition state because it is not a stationary point on the energy surface.[1]

(11) A reviewer expressed concern that the small differences in transition state energies might be meaningless in the context of the RRKM/phase space model of such reactions if the zero-point vibrational energies were significantly different for the different transition states. This is, however, not the case: the zero-point energies for the various transition states for the $CH_3CH{=}O/CH_2{=}CHO^-$ system differ by less than 0.35 kcal/mol; similarly, for the $CH_3CH{=}OH^+/CH_2{=}CHOH$ system they differ by less than 0.1 kcal/mol.

(12) For the hypothetical intermediates that define the corners 2, 3, 5, and 6 in Figure 3, the geometric parameters for the aldanionH^+ ($^-CH_2CH{=}OH^+$) are not included in Figures 1S[13] and 2S[13] because they are identical to those for $CH_3CH{=}OH^+$ except that one hydrogen is missing; for the enaldehydeH^+ ($^+HCH_2{=}CHOH$) the angles and bond lengths not explicitly indicated in Figures 1S[13] and 2S[13] are identical with those of the enol. Similar comments pertain to the aldanion ($^-CH_2CH{=}O$) and enaldehyde ($^+HCH_2{=}CHO^-$) in Figure 3S.[13]

(13) See the paragraph concerning supporting information at the end of this paper.

(14) Boys, S. F.; Bernardi, F. *Mol. Phys.* **1970**, *19*, 553.

(15) Davidson, E. R.; Chakravorty, S. J. *Chem. Phys. Lett.* **1994**, *217*, 48.

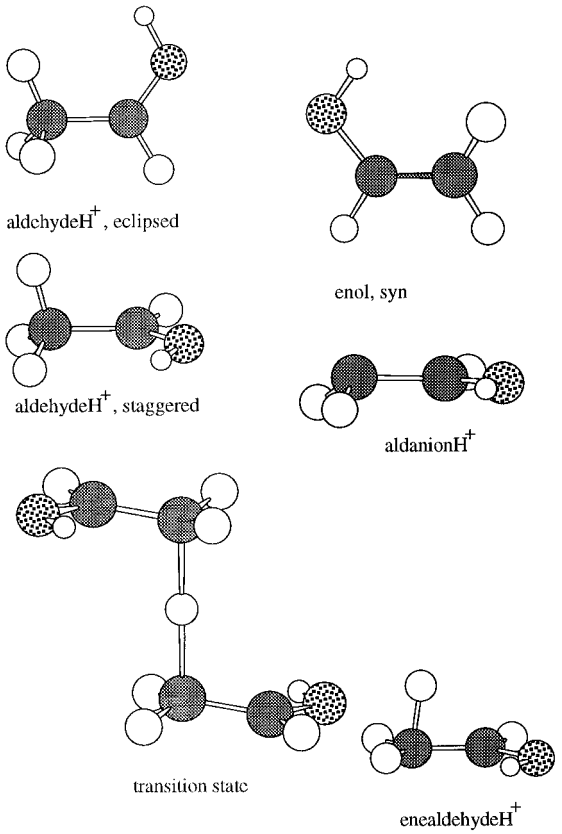

Figure 2. 3-D representations of the various structures relevant to the $CH_3CH{=}OH^+/CH_2{=}CHOH$ system (syn configuration).

The protonated aldehyde can exist in two configurations with respect to the OH proton: syn and anti relative to the methyl group. Furthermore, there are two conformations for each configuration: the eclipsed form in which one of the methyl hydrogens is eclipsed with the $C{=}OH^+$ group and the staggered form for which all methyl hydrogens are staggered with respect to the $C{=}OH^+$ group. The relative energies of the four isomers are anti, ecl < anti, stag ≤ syn, ecl < syn, stag, with the energy differences being 0.60, 0.14, and 0.66 kcal/mol, respectively.[16] For the neutral aldehyde we also have ecl < stag, with an energy difference of 0.36 kcal/mol.[16]

The enol can also exist in the syn and anti configurations. It is noteworthy that here it is the anti form that is of higher energy (1.57 kcal/mol).[16] The lower stability of the anti form of the enol was already noted by Wiberg et al.[17] and was attributed to a considerably higher dipole moment compared to that of the syn form.

With respect to the enthalpy of ionization, in the case of acetaldehyde a virtually perfect agreement is found between the calculated (368 kcal/mol) and the experimental (366 ± 2 kcal/mol)[18] values. Regarding the ΔH for the deprotonation of $CH_3CH{=}OH^+$ according to eq 5, there is no experimental quantity

$$CH_3CH{=}OH^+ \rightarrow CH_2{=}CHOH + H^+ \qquad (5)$$

for direct comparison because the loss of the carbon proton to yield the enol (eq 5) is less favorable than the loss of the oxygen proton to yield acetaldehyde (eq 6). However, since ΔH values for eq 6 (188.9 kcal/mol)[19] and eq 7 (11.2 kcal/mol)[20] are known

$$CH_3CH{=}OH^+ \rightarrow CH_3CH{=}O + H^+ \qquad (6)$$

$$CH_3CH{=}O \rightarrow CH_2{=}CHOH \qquad (7)$$

from experimental determinations, an "experimental" ΔH of 200.1 kcal/mol may be calculated for eq 5. This compares with 195.0 kcal/mol[16] for $CH_3CH{=}OH^+$ (anti, ecl) → $CH_2{=}CHOH$ (anti), 193.0 kcal/mol[16] for $CH_3CH{=}OH^+$ (syn, ecl) → $CH_2{=}CHOH$ (syn), 193.7 kcal/mol[16] for $CH_3CH{=}OH^+$ (anti, ecl) → $CH_2{=}CHOH$ (syn), and 194.3 kcal/mol[16] for $CH_3CH{=}OH^+$ (syn, ecl) → $CH_2{=}CHOH$ (anti). The agreement between any of the *ab initio* values and the experimental ΔH for eq 5 is clearly not as good as between the calculated and experimental gas phase enthalpies of deprotonation of acetaldehyde. Part of the discrepancies may arise from uncertainties in the experimental ΔH values for eqs 6[22] and 7.[21]

Transition State Structure. A. Charge Imbalance. Mulliken[24] as well as NPA[25] (natural population analysis) atomic charges for the various isomers of the protonated aldehyde, the enol, and the transition state have been calculated at the same three computational levels as the energies. The same holds for the aldehyde, enolate ion, and transition state of eq 1. They are summarized in Tables S2−S4[13] while the more relevant *group charges*,[1,9] which are used to evaluate the imbalance, are reported in Table 2.[26]

In calculating the imbalance in the acetaldehyde/enolate ion system, eq 2 was solved for n according to eq 8. Equations 2

$$n = \frac{\log(\delta_Y/\chi)}{\log(\delta_C + \delta_Y)} \qquad (8)$$

and 8 are equally applicable to the $CH_3CH{=}OH^+/CH_2{=}CHOH$ system even though the charge type is different and conforms to the generalized representation of eq 9 rather than eq 3. This

$$B + H{-}C{-}YH^+ \rightarrow \begin{bmatrix} \delta_B\ \ \delta_H\ \ -\delta_C\ \ 1-\delta_Y \\ B\text{- - -}H\text{- - -}C\text{---}YH \end{bmatrix}^{\ddagger} \rightarrow BH^+ + \begin{matrix} -1+\chi\ \ 1-\chi \\ C\text{---}YH \end{matrix} \qquad (9)$$

is because in both eqs 3 and 9, δ_Y and χ refer to the amount of negative charge that is being transferred to Y (or YH) upon reaching the transition state and product, respectively, regardless of whether or not there is a positive charge on YH to begin with.

On the basis of the above discussion, δ_Y and χ should correspond to 1 − (charge on $CHOH)_{TS}$ and 1 − (charge on $CHOH)_{enol}$, respectively, while δ_C should be equal to −(charge on CH_2) in the transition state. However, since in the protonated aldehyde the charge on the CHOH moiety is slightly less than

(16) Enthalpies determined at the MP2/6-311+G**//MP2/6-311+G** level.

(17) Wiberg, K. B.; Breneman, C. M.; LePage, T. J. *J. Am. Chem. Soc.* **1990**, *112*, 61.

(18) (a) Lias, S. G.; Bartmess, J. E.; Liebman, J. E.; Leoni, R. D.; Mallard, W. G. *J. Phys. Chem. Ref. Data* **1988**, *17*, Suppl 1. (b) Bartmess, J. E.; Scott, J. A.; McIver, R. I. *J. Am. Chem. Soc.* **1979**, *101*, 6046.

(19) Aue, D. H.; Bowers, M. T. In *Gas Phase Ion Chemistry*; Bauers, M. T., Ed.; Academic Press: San Francisco, 1979; Vol. 2, p 1.

(20) Tureček, F.; Brabec, L.; Korvola, J. *J. Am. Chem. Soc.* **1988**, *110*, 7984. This is considered the "best" value.[21]

(21) Apeloig, Y.; Arad, D.; Rappoport, Z. *J. Am. Chem. Soc.* **1990**, *112*, 9131.

(22) For a discussion of the uncertainties in the proton affinities, see ref 23.

(23) Moylan, C. R.; Brauman, J. I. *Annu. Rev. Phys. Chem.* **1983**, *34*, 187.

(24) See, e.g.: Hehre, W. J.; Radom, L.; Schleyer, P. v. R.; Pople, J. A. *Ab Initio Molecular Orbital Theory*; Wiley-Interscience: New York, 1986; p 25.

(25) (a) Glendenning, E. D.; Reed, A. E.; Carpenter, E.; Weinhold, F. NBO Version 3.1 in Gaussian 92 (ref 51). (b) Reed, A. E.; Curtiss, L. A.; Weinhold, F. *Chem. Rev.* **1988**, *88*, 899.

(26) It should be noted that the *atomic* charges (Tables S2−S4)[13] show a strong dependence on the computational level and particularly on the method (Mulliken vs NPA) but there is little variation in the *group* charges (Table 2).

Table 1. Ionization Energies, Reorganization Energies, and Reaction Barriers for Eqs 1 and 4

process	ΔE^d RHF[a]	ΔE^d MP2//RHF[b]	ΔE^d MP2//MP2[c]	$\Delta H^{d,e}$ RHF[a]	$\Delta H^{d,e}$ MP2//RHF[b]	$\Delta H^{d,e}$ MP2//MP2[c]
Eq 4 (Anti Configuration)						
$CH_3CH{=}OH^+$ (ecl) → $CH_2{=}CHOH$	210.88	202.56	202.54	203.39	195.07	195.04
$CH_3CH{=}OH^+$ (stag) → $CH_2{=}CHOH$	210.38	201.93	201.89	202.94	194.49	194.45
$CH_3CH{=}OH^+$ (ecl) → $^+HCH_2{=}CHOH$	27.87	21.94	22.74	26.95	21.02	21.82
$CH_3CH{=}OH^+$ (stag) → $^+HCH_2{=}CHOH$	27.38	21.31	22.09	26.51	20.44	21.22
$CH_2{=}CHOH$ → $^-CH_2CH{=}OH^+$	29.70	24.22	21.14	30.70	25.22	22.14
reactants (ecl) → TS	15.41	−3.68	−4.17	14.47	−4.62	−5.11
reactants (ecl) → TS_{corr}[f]	15.96	−1.33	−1.70	15.02	−2.27	−2.64
reactants (stag) → TS	14.92	−4.31	−4.82	14.03	−5.20	−5.71
reactants (stag) → TS_{corr}[f]	15.47	−1.96	−2.35	14.58	−2.85	−3.24
Eq 4 (Syn Configuration)						
$CH_3CH{=}OH^+$ (ecl) → $CH_2{=}CHOH$	208.70	200.38	200.33	201.34	193.02	192.97
$CH_3CH{=}OH^+$ (stag) $CH_2{=}CHOH$	208.12	199.69	199.62	201.81	192.39	192.31
$CH_3CH{=}OH^+$ (ecl) → $^+HCH_2{=}CHOH$	27.30	22.67	23.35	26.53	21.90	22.58
$CH_3CH{=}OH^+$ (stag) → $^+HCH_2{=}CHOH$	26.72	21.99	22.65	26.00	21.27	21.93
$CH_2{=}CHOH$ → $^-CH_2CH{=}OH^+$	31.22	25.68	22.64	30.51	24.97	21.93
reactants (ecl) → TS	17.90	−0.48	−0.80	16.78	−1.60	−1.92
reactants (ecl) → TS_{corr}[f]	18.44	1.78	1.60	17.32	0.66	0.48
reactants (stag) → TS	17.31	−1.16	−1.50	16.24	−2.23	−2.57
reactants (stag) → TS_{corr}[f]	17.85	1.10	0.90	16.78	0.03	−0.17
Eq 1						
$CH_3CH{=}O$ → $CH_2{=}CHO^-$	383.20	375.80	375.83	377.55	368.15	368.18
$CH_3CH{=}O$ (stag) → $CH_2{=}CHO^-$	382.70	374.99	375.36	375.16	367.45	367.82
$CH_3CH{=}O$ (ecl) → $^+HCH_2{=}CHO^-$	32.26	26.14	26.69	32.52	25.40	26.95
$CH_3CH{=}O$ (stag) → $^+HCH_2{=}CHO^-$	31.77	25.33	26.22	32.14	25.70	26.59
$CH_2{=}CHO^-$ → $^-CH_2CH{=}O$	13.35	13.44	10.85	13.13	13.21	10.62
reactants (ecl) → TS	16.34	1.02	0.17	16.46	1.14	0.29
reactants (ecl) → TS_{corr}[f]	16.92	3.92	3.20	17.04	4.04	3.32
reactants (stag) → TS	15.85	0.21	−0.30	16.08	0.44	−0.07
reactants (stag) → TS_{corr}[f]	16.43	3.11	2.73	16.66	3.34	2.96

[a] Optimized as restricted Hartree−Fock solution using 6-311+G**, i.e., 6-311+G**//6-311+G**. [b] MP2 performed at RHF geometry, i.e., MP2/6-311+G**//6-311+G**. [c] Optimized using MP2 gradients, i.e., MP2/6-311+G**//MP2/6-311+G**. [d] In kcal/mol. [e] At 298 K. [f] Corrected for BSSE.

+1 and the charge on the CH_3 group slightly larger than 0 (Table 2), we define δ_C as |(charge on $CH_2)_{TS}$ − (charge on $CH_3)_{aldehydeH^+}$], δ_Y as |(charge on $CHOH)_{TS}$ − (charge on $CHOH)_{aldehydeH^+}$|, and χ as |(charge on $CHOH)_{enol}$ − (charge on $CHOH)_{aldehydeH^+}$|, respectively. The calculated δ_C, δ_Y, and χ values for eq 4 are summarized in Table 3, along with the corresponding parameters for the aldehyde/enolate system (eq 1). The following points are noteworthy:

(1) Even though there is a trend toward lower *n* values with increasing computational level, the imbalance parameter is much larger than unity at all levels, regardless of the method (Mulliken or NPA) used, indicating a substantial transition state imbalance. In comparing different systems, we will focus on the *n* values obtained at the MP2/6-311+G**//MP2/6-311+G** level, but the comments made below are valid at all computational levels.

(2) In eq 4 for a given configuration (syn or anti) there is no significant dependence of *n* on the conformation of CH_3-$CH{=}OH^+$ (eclipsed vs staggered); the same is true for eq 1. On the other hand, in eq 4 *n* is significantly larger for the reaction of the syn isomers (Mulliken, 1.87−1.89; NPA, 1.72−1.73) than for the anti isomers (Mulliken, 1.68−1.71; NPA, 1.68−1.69). This result is consistent with the higher barrier in the reaction of the syn isomer as elaborated upon below.

(3) The *n* values for eq 4 are significantly larger than for eq 1, suggesting a greater imbalance in the $CH_3CH{=}OH^+$/$CH_2{=}CHOH$ system. One way to understand this result is in terms of the greater π-acceptor strength of the $CH{=}OH^+$ moiety compared to the CH=O moiety which may lead to a larger imbalance. This notion is supported by Saunders' [9b] *ab initio* study of the CH_3CN/CH_2CN^- system which shows a relatively small imbalance apparently because of the weak π-acceptor ability of the cyano group. It needs to be pointed out, though, that the theoretical framework in which we have viewed transition state imbalances and their consequences and manifestations[4,6] does not *require n* to increase with increasing π-acceptor strength of the Y group (eq 3).

In order to understand this assertion, one first needs to clarify how the term "imbalance" is being used. In solution proton transfers, imbalances are usually recognized by comparing Brønsted β_B values, obtained by varying the pK_a of a buffer base, with Brønsted α_{CH} values determined by varying the pK_a of the carbon acid through changes of remote substituents.[27] For reactions with imbalanced transition states, α_{CH} is typically larger than β_B[28] and the magnitude of $\alpha_{CH} - \beta_B$[32] is taken as an approximate measure of the imbalance. With $\alpha_{CH} - \beta_B$ as the definition of imbalance there is a direct correlation between imbalance and π-acceptor strength. This correlation is related

(27) For example, Z in $ZC_6H_4CH_2Y$.

(28) It is assumed that β_B is an approximate measure of charge or proton transfer at the transition state[29,30] although this view is not universally accepted.[31]

(29) Leffler, J. E.; Grunwald, E. *Rates and Equilibria of Organic Reactions*; Wiley: New York, 1963; p 156.

(30) (a) Kresge, A. J. *Acc. Chem. Res.* **1975**, *8*, 354. (b) Jencks, W. P. *Chem. Rev.* **1985**, *85*, 511.

(31) (a) Pross, A. *J. Org. Chem.* **1984**, *49*, 1811. (b) Bordwell, F. G.; Hughes, D. L. *J. Am. Chem. Soc.* **1985**, *107*, 4737. (c) Pross, A.; Shaik, S. S. *New J. Chem.* **1989**, *13*, 427.

(32) $\alpha_{CH} > \beta_B$ when the remote substituent, Z, is closer to the α-carbon than to the Y group, e.g., in $ZC_6H_4CH_2NO_2$ or $ZC_6H_4CH_2CH(CN)_2$. $\alpha_{CH} < \beta_B$ when the remote substituent is closer to the Y group than to the α carbon, e.g.,

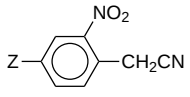

For a detailed discussion of these examples, see ref 4.

Table 2. Group Charges on Reactants, Products, and Transition States of Eqs 4 and 1

	RHF[a]		MP2//RHF[b]		MP2//MP2[c]	
group	Mulliken	NPA	Mulliken	NPA	Mulliken	NPA
			$CH_3CH{=}OH^+$ (Anti, Ecl)			
CHOH	0.820	0.374	0.813	0.857	0.809	0.851
CH_3	0.180	0.126	0.187	0.143	0.191	0.149
			$CH_3CH{=}OH^+$ (Anti, Stag)			
CHOH	0.810	0.875	0.805	0.859	0.801	0.853
CH_3	0.190	0.125	0.195	0.141	0.199	0.147
			$CH_3CH{=}OH^+$ (Syn, Ecl)			
CHOH	0.834	0.892	0.826	0.877	0.819	0.871
CH_3	0.166	0.108	0.174	0.123	0.181	0.129
			$CH_3CH{=}OH^+$ (Syn, Stag)			
CHOH	0.835	0.894	0.829	0.879	0.823	0.874
CH_3	0.165	0.106	0.171	0.121	0.177	0.126
			$CH_2{=}CHOH$ (Anti)			
CHOH	0.013	0.101	0.003	0.089	−0.002	0.086
CH_2	−0.013	−0.101	−0.003	−0.089	0.002	−0.086
			$CH_2{=}CHOH$ (Syn)			
CHOH	0.063	0.155	0.038	0.132	0.028	0.129
CH_2	−0.063	−0.155	−0.038	−0.132	−0.028	−0.129
			$CH_3CH{=}O$ (Ecl)			
CHO	0.049	0.021	0.055	0.026	0.052	0.021
CH_3	−0.049	−0.021	−0.055	−0.026	−0.052	−0.021
			$CH_3CH{=}O$ (Stag)			
CHO	0.035	0.023	0.044	0.029	0.039	0.022
CH_3	−0.035	−0.023	−0.044	−0.029	−0.039	−0.022
			$CH_2{=}CHO^-$			
CHO	−0.549	−0.480	−0.662	−0.521	−0.666	−0.531
CH_2	−0.451	−0.520	−0.338	−0.479	−0.334	−0.469
			TS (Anti), Eq 4			
CHOH	0.523	0.533	0.470	0.472	0.449	0.472
CH_2	−0.161	−0.212	−0.086	−0.134	−0.066	−0.132
H (transferred)	0.276	0.359	0.233	0.324	0.235	0.320
			TS (Syn), Eq 4			
CHOH	0.560	0.575	0.510	0.511	0.496	0.509
CH_2	−0.203	−0.254	−0.132	−0.172	−0.119	−0.170
H (transferred)	0.287	0.357	0.244	0.322	0.246	0.320
			TS, Eq 1			
CHO	−0.231	−0.200	−0.284	−0.245	−0.302	−0.266
CH_2	0.431	−0.470	−0.359	−0.404	−0.334	−0.384
H (transferred)	0.324	0.341	0.280	0.298	0.237	0.301

[a] Optimized as restricted Hartree−Fock solution using 6-311+G**, i.e., 6-311+G**//6-311+G**. [b] MP2 performed at RHF geometry, i.e., MP2/6-311+G**//6-311+G**. [c] Optimized using MP2 gradients, i.e., MP2/6-311+G**//MP2/6-311+G**.

to the fact that in the product ion the center of excess electron density is closer to Y and farther away from the remote substituent than in the transition state. This means that the effect of the remote substituent on the rate constant is disproportionately large compared to its effect on the acidity constant, and hence α_{CH} is exalted. Since the difference in the charge distribution between the transition state and the product ion increases with π-acceptor strength of Y, α_{CH} should also increase for a given degree of proton transfer (β_B)[28] at the transition state.

A different definition of imbalances can be formulated in terms of its effect on the intrinsic barrier of the reaction. This effect can be described by eq 10 where $\delta\Delta G^{\ddagger}_{o,res}$ is the change

$$\delta\Delta G^{\ddagger}_{o,res} = (\lambda_{res} - \beta_B)\delta\Delta G^{\circ}_{res} \qquad (10)$$

is $\Delta G^{\ddagger}_{o}$ (intrinsic barrier)[5] due to the change in the π-acceptor, $\delta\Delta G^{o}_{res}$ is the change in the free energy of the reaction caused by the change in resonance stabilization of the carbanion, β_B has the same meaning as above, and λ_{res} is a measure of resonance development at the transition state;[33] as shown below, λ_{res} is directly related to *n*. For a transition state in which resonance development lags behind proton transfer we have $\lambda_{res} < \beta_B$; hence, $|\lambda_{res} - \beta_B|$ can be regarded as a measure of imbalance. According to eq 10 the greater increase in $\Delta G^{\ddagger}_{o}$ [34] with increasing π-acceptor strength of Y can be solely explained by the increasingly more negative $\delta\Delta G^{\circ}_{res}$ and does not require the assumption of a larger $|\lambda_{res} - \beta_B|$, although a larger $|\lambda_{res} - \beta_B|$ may be a contributing factor.

That λ_{res} and $|\lambda_{res} - \beta_B|$ do not explicitly depend on the π-acceptor strength of Y can also be shown as follows.[35] If one assumes that resonance stabilization is proportional to the negative charge on Y, i.e., to χ in the product ion and to δ_Y in the transition state (eq 3), λ_{res} is given by eq 11, which in conjunction with eq 2, affords eq 12. Equation 12 shows that λ_{res} is not explicitly related to χ, and hence there is no requirement for λ_{res} to depend on the π-acceptor strength of Y.

(33) In previous papers,[4,6b] eq 10 was usually expressed in terms of rate and equilibrium constants instead of free energies, i.e., $\delta \log k^{res}_{o} = (\lambda_{res} - \beta_B)(\delta \log K^{res}_{1})$ where $\delta \log k^{res}_{o}$ is the change in the intrinsic rate constant and $\delta \log K^{res}_{1}$ the change in the equilibrium constant caused by the change in resonance stabilization of the carbanions. Both forms of the equation are of course equivalent.

(34) For a change to a Y group that is a stronger π-acceptor which implies $\delta\Delta G^{\circ}_{res} < 0$, $\delta\Delta G^{\ddagger}_{o,res} > 0$, i.e., $\Delta G^{\ddagger}_{o}$ is enhanced.

(35) For more details, see ref 4.

Table 3. Group Charge Differences and Imbalances

	RHF[a]		MP2//RHF[b]		MP2//MP2[c]	
parameter[d]	Mulliken	NPA	Mulliken	NPA	Mulliken	NPA
			Eq 4 (Anti Configuration)			
			$CH_3CH{=}OH^+$ (ecl) → $CH_2{=}CHOH$			
χ	0.807	0.773	0.810	0.768	0.811	0.765
$1-\chi$	0.193	0.227	0.190	0.232	0.189	0.235
$\chi/(1-\chi)$	4.18	3.41	4.26	3.31	4.29	3.26
			$CH_3CH{=}OH^+$ (stag) → $CH_2{=}CHOH$			
χ	0.796	0.774	0.802	0.769	0.803	0.768
$1-\chi$	0.204	0.226	0.198	0.231	0.197	0.232
$\chi/(1-\chi)$	3.90	3.42	4.05	3.33	4.08	3.31
			$CH_3CH{=}OH^+$ (ecl) → TS			
δ_Y	0.297	0.341	0.343	0.385	0.360	0.379
δ_C	0.340	0.338	0.273	0.277	0.257	0.281
$\delta_C+\delta_Y$	0.637	0.679	0.616	0.662	0.617	0.660
δ_Y/δ_C	0.874	1.009	1.256	1.390	1.401	1.349
n^e	2.22	2.12	1.78	1.68	1.68	1.69
$(\delta_Y/\delta_C)/[\chi/(1-\chi)]$	0.209	0.296	0.295	0.420	0.327	0.414
			$CH_3CH{=}OH^+$ (stag) → TS			
δ_Y	0.287	0.342	0.335	0.386	0.352	0.382
δ_C	0.351	0.337	0.281	0.276	0.265	0.279
$\delta_C+\delta_Y$	0.638	0.679	0.616	0.662	0.617	0.661
δ_Y/δ_C	0.817	1.015	1.192	1.399	1.328	1.369
n^e	2.27	2.11	1.80	1.67	1.71	1.68
$(\delta_Y/\delta_C)/[\chi/(1-\chi)]$	0.210	0.297	0.294	0.420	0.326	0.414
			Eq 4 (Syn Configuration)			
			$CH_3CH{=}OH^+$ (ecl) → $CH_2{=}CHOH$			
χ	0.771	0.738	0.789	0.746	0.791	0.742
$1-\chi$	0.229	0.262	0.211	0.254	0.209	0.258
$\chi/(1-\chi)$	3.37	2.82	3.74	2.94	3.78	2.88
			$CH_3CH{=}OH^+$ (stag) → $CH_2{=}CHOH$			
χ	0.772	0.739	0.791	0.747	0.795	0.745
$1-\chi$	0.228	0.261	0.209	0.253	0.205	0.255
$\chi/(1-\chi)$	3.39	2.83	3.78	2.95	3.88	2.92
			$CH_3CH{=}OH^+$ (ecl) → TS			
δ_Y	0.274	0.317	0.316	0.366	0.324	0.362
δ_C	0.369	0.362	0.306	0.295	0.300	0.299
$\delta_C+\delta_Y$	0.643	0.679	0.622	0.661	0.624	0.661
δ_Y/δ_C	0.743	0.876	1.033	1.241	1.080	1.211
n^e	2.34	2.18	1.93	1.72	1.89	1.73
$(\delta_Y/\delta_C)/[\chi/(1-\chi)]$	0.220	0.311	0.276	0.422	0.286	0.420
			$CH_3CH{=}OH^+$ (stag) → TS			
δ_Y	0.275	0.318	0.319	0.368	0.327	0.364
δ_C	0.368	0.360	0.303	0.293	0.296	0.296
$\delta_C+\delta_Y$	0.643	0.678	0.622	0.661	0.623	0.660
δ_Y/δ_C	0.747	0.883	1.053	1.256	1.105	1.230
n^e	2.34	2.17	1.91	1.71	1.87	1.72
$(\delta_Y/\delta_C)/[\chi/(1-\chi)]$	0.220	0.312	0.279	0.427	0.285	0.421
			Eq 1			
			$CH_3CH{=}O$ (ecl) → $CH_2{=}CHO^-$			
χ	0.598	0.501	0.717	0.547	0.718	0.552
$1-\chi$	0.402	0.499	0.282	0.453	0.282	0.448
$\chi/(1-\chi)$	1.488	1.004	2.533	1.207	2.546	1.232
			$CH_3CH{=}O$ (stag) → $CH_2{=}CHO^-$			
χ	0.585	0.503	0.706	0.549	0.705	0.554
$1-\chi$	0.415	0.497	0.294	0.451	0.295	0.446
$\chi/(1-\chi)$	1.410	1.012	2.401	1.217	2.390	1.242
			$CH_3CH{=}O$ (ecl) → TS			
δ_Y	0.280	0.221	0.339	0.271	0.354	0.287
δ_C	0.382	0.449	0.304	0.378	0.282	0.363
$\delta_C+\delta_Y$	0.662	0.670	0.643	0.649	0.636	0.650
δ_Y/δ_C	0.733	0.492	1.115	0.717	1.255	0.791
n^e	1.84	2.04	1.70	1.63	1.56	1.52
$(\delta_Y/\delta_C)/[\chi/(1-\chi)]$	0.493	0.490	0.440	0.594	0.493	0.642
			$CH_3CH{=}O$ (stag) → TS			
δ_Y	0.266	0.223	0.328	0.274	0.341	0.288
δ_C	0.396	0.447	0.315	0.375	0.295	0.362
$\delta_C+\delta_Y$	0.662	0.670	0.643	0.649	0.636	0.650
δ_Y/δ_C	0.672	0.499	1.041	0.731	1.156	0.796
n^e	1.91	2.03	1.74	1.62	1.60	1.51
$(\delta_Y/\delta_C)/[\chi/(1-\chi)]$	0.477	0.493	0.434	0.601	0.484	0.641

Footnotes for Table 3

[a] Optimized as restricted Hartree−Fock solution using 6-311+G**, i.e., 6-311+G**//6-311+G**. [b] MP2 performed at RHF geometry, i.e., MP2/6-311+G**//6-311+G**. [c] Optimized using MP2 gradients, i.e., MP2/6-311+G**//MP2/6-311+G**. [d] For the reaction of eq 4, the definition of the parameters is as follows: $\chi = |(\text{charge on CHOH})_{\text{enol}} - (\text{charge on CHOH})_{\text{aldehyde}^+}|$; $\delta_Y = |(\text{charge on CHOH})_{TS} - (\text{charge on CHOH})_{\text{aldehyde}^+}|$; $\delta_C = |(\text{charge on CH}_2)_{TS} - (\text{charge on CH}_3)_{\text{aldehyde}^+}|$. For the reaction of eq 1 the definition of the parameters is as follows: $\chi = |(\text{charge on CHO})_{\text{enolate}} - (\text{charge on CHO})_{\text{aldehyde}}|$; $\delta_Y = |(\text{charge on CHO})_{TS} - (\text{charge on CHO})_{\text{aldehyde}}|$; $\delta_C = |(\text{charge on CH}_2)_{TS} - (\text{charge on CH}_3)_{\text{aldehyde}}|$. [e] *n* calculated from eq 8.

$$\lambda_{res} = \delta_Y/\delta_\chi \tag{11}$$

$$\lambda_{res} = (\delta_C + \delta_Y)^n \tag{12}$$

However, λ_{res} may depend *indirectly* on π-acceptor strength if *n* is a function of the latter; the increase in *n* from the CH_3CN/CH_2CN^- system to the $CH_3CH{=}O/CH_2{=}CHO^-$ and $CH_3CH{=}OH^+/CH_2{=}CHOH$ systems implies that this is the case.

B. Geometries. Further insights into the transition state structure can be obtained from certain geometrical parameters. For example, the pyramidal angle shown in **1** (X = H or lone

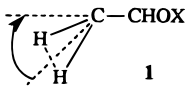

1

pair) may be regarded as an approximate measure of pyramidalization of the α-carbon. Values for these angles in $CH_3CH{=}OH^+$, $CH_3CH{=}O$, and the respectively transition states are summarized in Table 4. For both eqs 4 and 1 pyramidalization at the transition state is still extensive which suggests that the α-carbon has retained a considerable degree of sp^3 character. This is consistent with the large fraction of the negative charge residing on the α-carbon of the transition state.

Table 4 also reports the fractional change in the pyramidal angle upon reaching the transition state. It is not clear whether the degree by which this angle has changed at the transition state has any quantitative relationship to the imbalance. This is because the relationship between the charge on the CH_2 fragment and pyramidalization is undoubtedly a complex one since sp^3 hybridization is not a prerequisite for the α-carbon to be able to carry a partial negative. This can be seen, e.g., from the significant amount of charge on the CH_2 fragment in the completely planar enolate ion. Nevertheless, it is noteworthy that, except for the reactions of $CH_3CH{=}OH^+$ in the eclipsed conformation, the fractional change of the pyramidal angle at the transition state is significantly less than 0.5, consistent with the charge imbalance. The much larger decrease (fractional change of ∼0.5) in the pyramidal angle for the reactions of the eclipsed $CH_3CH{=}OH^+$ conformers may, to a significant extent, be an artifact caused by abnormally large pyramidal angles of about 60° in $CH_3CH{=}OH^+$; as a point of reference, the pyramidal angle in methane is 54.73°.

Another perspective on structural changes that arise upon reaching the transition state is obtained from the C—C and C—O bond lengths. They are summarized in Table 5 for eq 4 and Table 6 for eq 1. Included in the tables are the fractional bond changes that have occurred upon reaching the transition state. For example, for the eclipsed conformers of $CH_3CH{=}OH^+$, they are $\Delta r^{\ddagger}_{CC}/\Delta r^{\circ}_{CC} \approx 0.64$ (anti) and ≈ 0.63 (syn) for the C—C bond, and $\Delta r^{\ddagger}_{CO}/\Delta r^{\circ}_{CO} \approx 0.47$ (anti) and ≈ 0.46 (syn) for the C—O bond. The $\Delta r^{\ddagger}_{CC}/\Delta r^{\circ}_{CC}$ ratios are close to the *total* negative charge generated at the transition state, i.e., $\delta_C + \delta_Y$ (Table 3), and much larger than the charge generated on the CHOH moiety, i.e., δ_Y (Table 3). The same is true for $\Delta r^{\ddagger}_{CC}/\Delta r^{\circ}_{CC}$ in eq 1. These results are consistent with the model underlying eq 2,[1,36] as elaborated upon previously.[1]

(36) See in particular eq 5 of ref 1.

Table 4. Pyramidal Angles in Reactants and Transition States of Eqs 4 and 1[a]

	pyramidal angle[b] (deg)		fractional change[c]
	reactant	TS	
$CH_3CH{=}OH^+$ (anti, ecl)	60.12	30.08	0.500
$CH_3CH{=}OH^+$ (anti, stag)	48.03	30.08	0.393
$CH_3CH{=}OH^+$ (syn, ecl)	60.36	29.79	0.494
$CH_3CH{=}OH^+$ (syn, stag)	48.73	29.79	0.373
$CH_3CH{=}O$ (ecl)	51.55	37.32	0.276
$CH_3CH{=}O$ (stag)	56.26	37.32	0.337

[a] Calculated at the MP2/6-311+G**//MP2/6-311+G** level. [b] The pyramidal angle of the enol (enolate ion) product is 0. [c] Defined as {angle(reactant) − angle(TS)}/angle(reactant).

Reaction Barriers. We shall use the term "barrier" for the enthalpy differences between the transition state and reactants rather than for the enthalpy difference between the transition state and the ion−dipole complex that typically lies between reactants and the transition state on the reaction coordinates of gas phase ion−molecule reactions.[23,37] This means that when the transition state is of lower energy than the reactants the barrier is negative. The ion−dipole complexes are of interest in their own right, but their enthalpies are mainly determined by attractive forces between the reactants, and in some cases the orientation of the two species within the complex bears little similarity to that in the transition state.[9] Hence, they have little relevance to the main focus of this paper which is the difference in structure and energy between transition states and reactants, and no attempt has been made to include them in our calculations.

The barriers are summarized in Table 1 for both eqs 4 and 1. Values with and without counterpoise corrections for the BSSE[14] are reported. It is noteworthy that the corrections are larger at the MP2 levels compared with the RHF level, in agreement with findings by Mó et al.[38] for protonation energies. However, at a given computational level the BSSE corrections depend little on the specific reaction: e.g., for the two $CH_3CH{=}OH^+/CH_2{=}CHOH$ systems at the MP2/6-311+G**//MP2/6-311+G** level they are 2.47 kcal/mol for the anti and 2.40 kcal/mol for the syn configuration, while for the $CH_3CH{=}O/CH_2{=}CHO^-$ system at the same level the correction amounts to 3.03 kcal/mol. Hence, in comparing barriers for the different systems, the discussion can be based on either the corrected or uncorrected values.

In response to a concern expressed by a reviewer, the intrinsic reaction coordinate was followed using GAMESS[39] to determine whether the computed transition state was truly a maximum after BSSE corrections. For displacements along the normal mode of the imaginary mode, energy does decrease. The BSSE correction computed for points close to the transition state also

(37) (a) Farneth, W. E.; Brauman, J. I. *J. Am. Chem. Soc.* **1976**, *98*, 7891. (b) Pellerite, M. J.; Brauman, J. I. *J. Am. Chem. Soc.* **1980**, *102*, 5993.

(38) Mó, O.; de Paz, J. L. G.; Yáñez, M. *Theor. Chim. Acta* **1988**, *73*, 307.

(39) Schmidt, M. W.; Baldridge, K. K.; Boatz, J. A.; Elbert, S. T.; Gordon, M. S.; Jensen, J. H.; Koseki, S.; Matsunaga, N.; Nguyen, K. A.; Su, S. J.; Windus, T. L.; Dupuis, M.; Montgomery, J. A. *J. Comput. Chem.* **1993**, *14*, 1347−1363.

Table 5. C—C and C—O Bond Lengths in Reactants, Products, and the Transition State of Eq 4[a]

bond	$CH_3CH{=}OH^+$ (ecl)	$CH_3CH{=}OH^+$ (stag)	$CH_2{=}CHOH$	TS
		Anti Configuration		
r_{CC}	1.455	1.458	1.337	1.380
r_{CO}	1.264	1.265	1.369	1.314
Δr°_{CC} (ecl)[b]			−0.118	
Δr°_{CC} (stag)[b]			−0.121	
$\Delta r^\ddagger_{CC}$ (ecl)[c]				−0.075
$\Delta r^\ddagger_{CC}$ (stag)[c]				−0.078
Δr°_{CO} (ecl)[b]			0.105	
Δr°_{CO} (stag)[b]			0.104	
$\Delta r^\ddagger_{CO}$ (ecl)[c]				0.050
$\Delta r^\ddagger_{CO}$ (stag)[c]				0.049
$\Delta r^\ddagger_{CC}/\Delta r^\circ_{CC}$ (ecl)				0.636
$\Delta r^\ddagger_{CC}/\Delta r^\circ_{CC}$ (stag)				0.645
$\Delta r^\ddagger_{CO}/\Delta r^\circ_{CO}$ (ecl)				0.476
$\Delta r^\ddagger_{CO}/\Delta r^\circ_{CO}$ (stag)				0.471
		Syn Configuration		
r_{CC}	1.461	1.464	1.340	1.385
r_{CO}	1.262	1.262	1.363	1.309
Δr°_{CC} (ecl)[b]			−0.121	
Δr°_{CC} (stag)[b]			−0.124	
$\Delta r^\ddagger_{CC}$ (ecl)[c]				−0.076
$\Delta r^\ddagger_{CC}$ (stag)[c]				−0.079
Δr°_{CO} (ecl)[b]			0.101	
Δr°_{CO} (stag)[b]			0.101	
$\Delta r^\ddagger_{CO}$ (ecl)[c]				0.047
$\Delta r^\ddagger_{CO}$ (stag)[c]				0.047
$\Delta r^\ddagger_{CC}/\Delta r^\circ_{CC}$ (ecl)				0.628
$\Delta r^\ddagger_{CC}/\Delta r^\circ_{CC}$ (stag)				0.637
$\Delta r^\ddagger_{CO}/\Delta r^\circ_{CO}$ (ecl)				0.465
$\Delta r^\ddagger_{CO}/\Delta r^\circ_{CO}$ (stag)				0.465

[a] In angstroms, calculated at the MP2/6-311+G**//MP2/6-311+G** level. [b] $\Delta r^\circ = r$(enol) − $r(CH_3CH{=}OH^+)$. [c] $\Delta r^\ddagger = r$(TS) − $r(CH_3CH{=}OH^+)$.

Table 6. C—C and C—O Bond Lengths in Reactants, Products, and the Transition State of Eq 1[a]

bond	$CH_3CH{=}O$ (ecl)	$CH_3CH{=}O$ (stag)	$CH_2{=}CHO^-$	TS
r_{CC}	1.505	1.508	1.390	1.416
r_{CO}	1.215	1.215	1.271	1.246
Δr°_{CC} (ecl)[b]			−0.115	
Δr°_{CC} (stag)[b]			−0.118	
$\Delta r^\ddagger_{CC}$ (ecl)[c]				−0.089
$\Delta r^\ddagger_{CC}$ (stag)[c]				−0.092
Δr°_{CO} (ecl)[b]			0.056	
Δr°_{CO} (stag)[b]			0.056	
$\Delta r^\ddagger_{CO}$ (ecl)[c]				0.031
$\Delta r^\ddagger_{CO}$ (stag)[c]				0.031
$\Delta r^\ddagger_{CC}/\Delta r^\circ_{CC}$ (ecl)				0.774
$\Delta r^\ddagger_{CC}/\Delta r^\circ_{CC}$ (stag)				0.780
$\Delta r^\ddagger_{CO}/\Delta r^\circ_{CO}$ (ecl)				0.554
$\Delta r^\ddagger_{CO}/\Delta r^\circ_{CO}$ (stag)				0.554

[a] In angstroms, calculated at the MP2/6-311+G**//MP2/6-311+G** level. [b] $\Delta r^\circ = r$(enolate ion) − r(aldehyde). [c] $\Delta r^\ddagger = r$(TS) − r(aldehyde).

decreases with increasing displacement from the transition state. Hence, the calculated transition states indeed appear to be maxima on the potential energy surfaces for the reactions discussed. This is not surprising because our reactions are identity reactions and the principle of microscopic reversibility requires the transition state to be symmetrical in the sense that the proton is equidistant between the two fragments.

The differences between the intrinsic barriers of the various reactions are probably the result of a complex interplay of at least three known factors.[40] One is the expected increase in the barrier with increasing imbalance. The second factor is a trend toward lower barriers with increasing acidity of the proton donor, as demonstrated by Scheiner et al.,[41] and recently confirmed by Saunders et al.[9b] when comparing barriers of the CH_4/CH_3^-, $CH_2{=}CH_2/CH_2{=}CH^-$, and $HC{\equiv}CH/HC{\equiv}C^-$ systems. The same kind of correlation between acidity and barriers has also been noted by Gronert[42] in his *ab initio* study of the identity proton transfer from first- and second-row non-metal hydrides to their conjugate bases; in solution, a similar phenomenon has been reported for the identity proton transfer of transition metal hydride complexes $CpM(CO)_3H$.[43] The third factor is the electrostatic or hydrogen bonding interaction between the positively charged transferred proton and the CH_2

(40) Saunders et al.[9b] report that polarizability effects may be important in some cases.

(41) (a) Cybulski, S. M.; Scheiner, S. *J. Am. Chem. Soc.* **1987**, *109*, 4199. See also: Scheiner, S.; Wang, L. *J. Am. Chem. Soc.* **1992**, *114*, 3650. (b) Scheiner, S. *J. Mol. Struct.*: *THEOCHEM* **1994**, *307*, 65.

(42) Gronert, S. *J. Am. Chem. Soc.* **1993**, *115*, 10258.

(43) Eididin, R. J.; Sullivan, J. M.; Norton, J. R. *J. Am. Chem. Soc.* **1987**, *109*, 3945.

fragments at the transition state: this interaction leads to a stabilization of the transition state which should increase with increasing positive charge on the transferred proton and/or increasing negative charge on the CH_2 fragments. Strong evidence for the importance of this effect comes from the comparison of the constrained trans-anti TS with the optimized cis-gauche TS in the $CH_3CH{=}O/CH_2{=}CHO^-$ [1] alluded to in the Introduction.

In comparing the reactions of the different isomers of $CH_3CH{=}OH^+$, we note that at the MP2/6-311+G**//MP2/6-311+G** level the barriers for the syn isomers (ΔH(ecl) = −1.92 kcal/mol *vs* ΔH(stag) = −2.57 kcal/mol, or $\Delta H(\text{ecl})_{\text{corr}}$ = 0.48 kcal/mol *vs* $\Delta H(\text{stag})_{\text{corr}}$ = −0.17 kcal/mol) are significantly higher (less negative) than for the anti isomers (ΔH(ecl) = −5.11 kcal/mol *vs* ΔH(stag) = −5.71 kcal/mol, or $\Delta H(\text{ecl})_{\text{corr}}$ = −2.64 kcal/mol *vs* $\Delta H(\text{stag})_{\text{corr}}$ = −3.24 kcal/mol). Of the factors identified above, only the larger imbalance associated with the syn isomers can explain the higher barrier for these isomers. The slightly higher acidity of the syn isomers would lower the barrier, and the same is expected for the larger electrostatic interaction between the transferred proton and the somewhat more negative α-carbons in the syn transition state. Apparently the barrier-increasing effect of the larger imbalance outweighs the other two factors.

The above situation is reversed when eq 4 is compared with eq 1: Here the much higher acidity of $CH_3CH{=}OH^+$ compared to $CH_3CH{=}O$ is the dominant factor. It leads to lower barriers for eq 4 (e.g., $\Delta H_{\text{anti,ecl}}$ = −5.11 kcal/mol, $\Delta H_{\text{syn,ecl}}$ = −1.92 kcal/mol) than for eq 1 (e.g., ΔH_{ecl} = 0.29 kcal/mol), despite competition by three barrier-enhancing factors. These are the larger *n* value for eq 4, the greater π-acceptor strength of the $CH{=}OH^+$ group compared to the CH=O group (more negative $\delta\Delta G^{\ddagger}_{\text{o,res}}$ [44] in eq 10), and the much reduced electrostatic or hydrogen-bonding stabilization resulting from the much smaller charges on the transferred proton and the CH_2 fragments at the transition state of eq 4. The dominance of the acidity factor is also seen in the comparison between reactions starting with the staggered and those starting with the eclipsed conformation for both eqs 1 and 4: here the differences in the barriers are very small, reflecting very small differences in the acidities and negligible differences in the imbalances.

The barrier-lowering effect of the higher acidity of the CH acid has been attributed to a stronger attraction between the proton donor and acceptor which reduces the distance between the proton donor and acceptor atom at the transition state, thereby allowing the proton to move a shorter distance.[41] The fact that the C- - -H- - -C distance is reduced from 2 × 1.416 Å in eq 1 to 2 × 1.410 Å (syn) and 2 × 1.401 Å (anti) in eq 4[45] is consistent with Scheiner's findings. Another, probably more important, factor is the inductive/field effect that is responsible for the higher acidity.[47]

(44) It is reasonable to expect that the entropy terms of the various reactions are very similar or identical and hence eq 10 is equally valid for enthalpies.

(45) In comparing the cis-gauche transition state with the constrained trans-anti transition state in the $CH_3CH{=}O/CH_2{=}CHO^-$ system,[1] we also noted that the more stable cis-gauche transition state has a shorter C- - -H- - -C distance (2 × 1.447 Å)[46] than the constrained trans-anti transition state (2 × 1.484 Å).[46] In this case a stronger electrostatic effect, due to a larger positive charge on the proton and a larger negative charge on the CH_2 groups, is probably the underlying reason for both the shorter C- - -H- - -C distance and greater stability of the cis-gauche transition state. Such an electrostatic effect cannot be invoked to explain the lower energy of the transition state of eq 4 compared to that of eq 1 because the charges on the proton and on the CH_2 groups are *smaller* in the transition state of eq 4 compared to that of eq 1.

(46) These C- - -H- - -C distances were calculated at the MP2/6-311+G**//6-311+G** rather than the MP2/6-311+G**//MP2/6-311+G** level.[1]

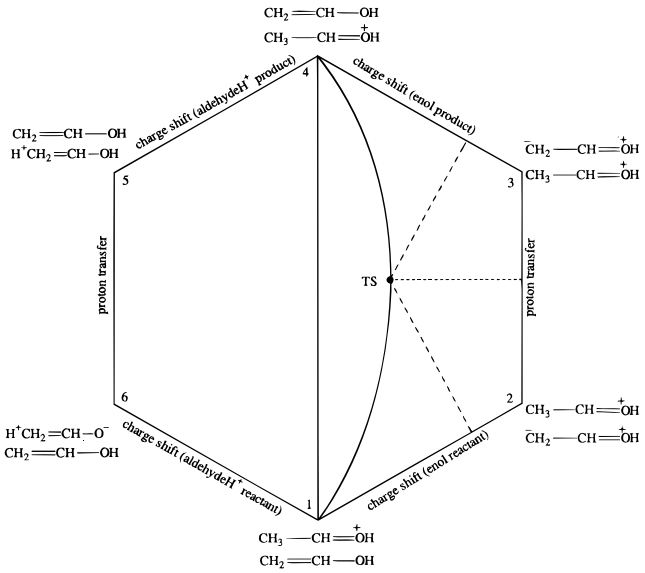

Figure 3. More O'Ferrall−Jencks diagram with separate axes for proton transfer and charge shifts, illustrating the imbalance between proton transfer and charge shift in eq 4.

More O'Ferrall−Jencks Diagram. In dealing with the $CH_3CH{=}O/CH_2{=}CHO^-$ system, we showed that eq 1 can be represented by a six-corner More O'Ferrall[48]−Jencks[3,49] type diagram with separate axes for proton transfer and charge shift. A similar diagram for eq 4 is shown in Figure 3. Corners 1 and 4 are the reactants and products, respectively. Corners 2 and 3 are hypothetical states in which the enol has undergone a shift in π-electrons from the C−O bond to the C−C bond, creating the resonance structure **2**; in analogy to the structure in the $CH_3CH{=}O/CH_2{=}CHO^-$ system, **3**, which was named "aldanion", we call **2** "aldanionH^+".

$^-CH_2{-}CH{=}OH^+$ **2** $\qquad$ $^-CH_2{-}CH{=}O$ **3**

Corners 5 and 6 are hypothetical states in which the protonated aldehyde has undergone a shift in electrons from a C−H bond to the C−O bond, creating the resonance structure **4**; we call it "enaldehydeH^+", in analogy to "enaldehyde" for structure **5** in the $CH_3CH{=}O/CH_2{=}CHO^-$ system.

$H^+CH_2{=}CH{-}OH$ **4** $\qquad$ $H^+CH_2{=}CH{-}O^-$ **5**

Figure 3 defines three hypothetical limiting reaction pathways of interest. The first is a stepwise reaction via corners 2 and 3. It starts with a π-electron shift in the *reactant* enol to form **2**; it is followed by proton transfer and finally by a π-electron shift to transform the product aldanionH^+ into the *product* enol. The second is a stepwise pathway via corners 6 and 5; here there is a charge shift in the *reactant* $CH_3CH{=}OH^+$ to form **4**, followed by proton transfer and transformation of the product enaldehydeH^+ into the *product* $CH_3CH{=}OH^+$. The third limiting pathway is a concerted, synchronous pathway represented by the vertical line connecting corners 1 and 4; its transition state is in the center of the diagram where proton transfer as well as charge reorganization has made 50% progress.

As our charge calculations imply, the *actual* pathway is concerted but not synchronous; i.e., the charge shift in the enol

(47) Bernasconi, C. F.; Wenzel, P. J.; Keeffe, J. R.; Gronert, S. To be published.

(48) More O'Ferrall, R. A. *J. Chem. Soc. B* **1970**, 274.

(49) Jencks, W. P. *Chem. Rev.* **1972**, *72*, 705.

reactant is ahead and the charge shift in the enol product lags behind proton transfer. This requires placement of the transition state inside the right half of the diagram; due to the symmetry of the reaction, the transition state must be equidistant from corners 1 and 4. The imbalance is clearly seen by projecting the reaction coordinate onto the enol charge-shift and proton-transfer axes.

An examination of the energies of **2** and **4** is revealing; they were obtained as follows. For the aldanionH^+, **2**, a structure was assumed which has the optimized geometry of $CH_3CH{=}OH^+$ except that the proton perpendicular to the $CH{=}OH^+$ group has been removed. For the enaldehydeH^+, **4**, we assumed a structure in which the enol geometry is enforced, a proton is added, and the position of this proton is optimized.

The ΔH values for the conversion of $CH_3CH{=}OH^+$ into **4** and the enol into **2** are summarized in Table 1 (absolute energies are in Table S1);[13] they correspond to the energy levels of corners 5 and 6, and 2 and 3, respectively, relative to corners 1 and 4. The intermediate corners are seen to be of comparable energy and about 21−22 kcal/mol[16] above the reactant/product corners. This compares with ∼26.5 kcal/mol for corresponding corners 5 and 6 (**5**) and ∼10.5 kcal/mol for the corresponding corners 2 and 3 (**3**) in the $CH_3CH{=}O/CH_2{=}CHO^-$ system. The increase in energy required to convert the enol into **2** compared to the energy to convert the enolate ion into **3** may, at least in part, be due to the need for charge *creation* and *separation* in the former whereas in the latter there is only a charge *redistribution*. The reduction in energy required in the conversion of $CH_3CH{=}OH^+$ into **4** compared to the energy for the conversion of the neutral aldehyde into **5** may be explained in a similar way; i.e., conversion of $CH_3CH{=}OH^+$ into **4** only involves charge redistribution rather than charge creation and separation.

The consequence of the changes in the relative energies of the intermediate corners when eq 4 is compared with eq 1 is that the downward tilt from the left to the right hand side which characterized the corresponding diagram for the $CH_3CH{=}O/CH_2{=}CHO^-$ system essentially disappears in the diagram for the $CH_3CH{=}OH^+/CH_2{=}CHOH$ system, implying a more symmetrical energy surface for the latter reaction. On the basis of this reasoning, one might expect the reaction coordinate to be close to the center and hence the transition state to be less imbalanced than for eq 1. This notion, however, conflicts with the conclusions reached based on charge distributions. Apparently, similarity of the energies of the intermediate corner does not necessarily imply a symmetric energy surface; i.e., the relative energies of the intermediate corners are not always a good predictor of transition state imbalances.

This lack of correlation between the expected changes in the energy surface and the observed imbalances is most likely a consequence of comparing two systems whose electronic structures are too different to permit treatment of the change from eq 1 to eq 4 as a "small perturbation". On the other hand, when the reactions of the syn and anti $CH_3CH{=}OH^+/CH_2{=}CHOH$ systems are compared, a comparison which does qualify as a small perturbation, we do see the expected correlation between *n* and the relative energies of the intermediate corners: For the anti system, corners 2 and 3 (22.14 kcal/mol) are slightly higher than corners 5 and 6 (ecl, 21.82 kcal/mol; stag, 21.22 kcal/mol) while for the syn system corners 2 and 3 (21.93 kcal/mol) are slightly lower than or the same as corners 5 and 6 (ecl, 22.58 kcal/mol; stag, 21.93 kcal/mol). This suggests that the position of the transition state for the syn system is to the right of that of the anti system, consistent with a larger imbalance for the syn system.

Methods

Optimizations, force field calculations, and Moeller−Plesset[50] calculations were carried out using the GAUSSIAN 92 suites of programs.[51] The standard basis sets (6-311) were used with diffuse (+) and polarization functions (d on second row, p on hydrogen atoms) described by Pople.[52] Optimizations were performed with MP2 gradients at 6-311+G** with SCF=DIRECT. Since force fields could not be practically computed for the transition states, the force fields at RHF/6-311+G** optimized geometries were used, scaled by 0.905 in accordance with our work on the acetaldehyde system;[1] the zero-point energy corrections are reported for 298 K.

BSSE Correction. The basis set superposition error (BSSE) is estimated for the transition state structures using the counterpoise method of Boys and Bernardi.[14] The transition state is treated as two separate fragment monomers. One includes the transferred proton; the other does not. The counterpoise correction is estimated for each fragment and summed to give the transition state correction.

To determine the variability of the BSSE as a function of displacement along the reaction coordinate, an intrinsic reaction path is followed using GAMESS[39] at the RHF/6-311+G** theoretical level. The BSSE was evaluated at points separated by less than 2 kcal/mol of the transition state energy to demonstrate that the BSSE falls as the displacement away from the transition state structure increases.

Syn Transition State. Using the fully optimized coordinates for the trans-anti transition state from the $CH_3CH{=}O/CH_2{=}CHO^-$ system, a proton was added to the oxygen atom. These coordinates were then optimized at RHF/6-311+G**, and the force field evaluated. The optimized coordinates were then the starting point for optimization at MP2/6-311+G**. In each of these cases the SCF=Direct option was employed. The optimizations were then repeated using Cartesian coordinates again using the direct method. The internally optimized coordinates were unchanged using Cartesian coordinates at both levels;[1] the zero-point energy corrections are reported for 298 K.

Anti Transition State. From the RHF/6-311+G** optimized syn transition state the relative position of the hydroxyl proton was inverted. These coordinates were then reoptimized at RHF/6-311+G**. The resulting coordinates were then the starting point for the MP2/6-311+G** optimizations. The SCF=Direct option was chosen for both the RHF and MP2 optimizations. As in the syn case, optimization in Cartesian coordinates left the result for internal coordinates unchanged. We conclude that no unforeseen constraints or coordinate couplings were introduced in the defined internal coordinates used.

AldanionH^+ and EnolateH^+. The aldanionH^+ (**2**) structures (syn and anti) refer to the protonated aldehyde staggered structures optimized at 6-311+G**, the staggered proton removed, and the force field computed at this level. At MP2 the appropriate optimized geometry, less staggered proton, were run as single point calculations.

The enaldehydeH^+ (**4**) is the enol (syn or anti) with coordinates fixed while the coordinates for an added proton were computed. This was done at RHF/6-311+G**. The force fields were then computed. At these geometries the MP2 energy was also computed; we report this as MP2/6-311+G**//6-311+G**. Additionally we have optimized a proton at MP2 using the MP2 geometries of the corresponding enols. These are reported at MP2/6-311+G**//MP2/6-311+G**.

Trans−Anti Aldehyde Transition State. A **Z** matrix was constructed exploiting the symmetry of the transition state. Variables were assigned such that the transferred proton represented a point of inversion for each assigned parameter in the structure. The initial values were those of our previously published cis-gauche transition state.[1] During optimization at MP2/6-311+G** the symmetry was turned off to allow

(50) (a) Moeller, C.; Plesset, M. S. *Phys. Rev.* **1934**, *46*, 618. (b) Krishnan, R.; Pople, J. A. *Int. J. Quantum Chem.* **1978**, *14*, 91. (c) Krishnan, R.; Frisch, M. J.; Pople, J. A. *J. Chem. Phys.* **1980**, *72*, 4244. (d) Frisch, M. J.; Head-Gordon, M.; Pople, J. A. *Chem. Phys. Lett.* **1990**, *166*, 281.

(51) Frisch, M. J.; Trucks, G. W.; Head-Gordon, M.; Gill, P. M. W.; Wong, M. W.; Foresman, J. B.; Johnson, B. G.; Schlegel, H. B.; Robb, M. A.; Replogle, E. S.; Gomperts, R.; Andres, J. L.; Raghavachari, K.; Binkley, J. S.; Gonzalez, C.; Martin, R. L.; Fox, D. J.; DeFrees, D. J.; Baker, J.; Stewart, J. J. P.; Pople, J. A. *GAUSSIAN 92*, Revision B; Gaussian, Inc.: Pittsburgh, PA, 1992.

(52) Hehre, W. J.; Radom, L.; Schleyer, P. v. R.; Pople, J. A. *Ab Initio Molecular Orbital Theory*; Wiley-Interscience: New York, 1986.

the transition state to rotate freely about the axis defined by the transferred proton. No such rotation occurred, and the structure was optimized such that it belongs to the C_i symmetry point group.[53] This structure is similar to that published by Saunders.[9a]

Acknowledgment. This work has been supported by Grant No. CHE-9307659 from the National Science Foundation. Additional support was provided by NSF grants through the San Diego Supercomputing Center on the CRAY C90, account numbers CSC202 and CSC651, and through the Pittsburgh Computing Center on the Cray YMP/832, Grant No. CH#920015P. We are also indebted to Professor Scott Gronert for critical discussion, and to Professor William H. Saunders, J., for providing us with unpublished results.

Supporting Information Available: Tables S1−S4, energies and atomic charges, and Figures S1−S3, geometric parameters (11 pages). See any current masthead page for ordering and Internet access instructions.

JA960233J

(53) Cotton, F. A. *Chemical Applications of Group Theory*, 3rd ed.; Wiley & Sons: New York, 1990; p 22.